# High-Contrast, Narrow-Field Imaging with a Fiber-Coupled Multi-Aperture Telescope

Gene Serabyn
Jet Propulsion Laboratory, MS 171-113
California Institute of Technology, Pasadena, CA 91109
gene.serabyn@jpl.nasa.gov

*Abstract*—The direct detection of faint planets around bright nearby stars calls for the development of high-contrast narrow-field detection techniques. A number of novel coronagraphs have recently been proposed, but this challenging goal may also call for the development of novel types of telescope architecture. The approach to high-contrast narrow-field imaging presented here replaces the monolithic telescope assembly with an array of small "sub-aperture" telescopes, with the final pupil being assembled by means of a single-mode fiber array. Such an approach can potentially have a much smaller volume, mass and cost than a large and accurately-figured monolithic telescope.

## 1. INTRODUCTION

Imaging nearby planetary systems requires high angular-resolution, high contrast observations very close to bright stars. To image a sizable number of potential systems, stars out to a few tens of parsecs must be observable with a given technique. For example, at a distance of 20 pc, a radius of 1 AU subtends 50 milli arcsec (mas), so the angular resolution must be of this order or better. In terms of the wavelength, $\lambda$, and aperture diameter, D, the full width at half maximum (FWHM) angular resolution of a single, round telescope aperture is approximately $\lambda/D$. Numerically, with $\lambda_{\mu m}$ the wavelength in microns and $D_m$ the aperture diameter in meters,

$$\text{FWHM} \approx \frac{l}{D} \approx 200 \frac{l_{mm}}{D_m} \text{ mas.} \qquad (1)$$

A resolution of 50 mas with a single round aperture then implies $D_m \approx 4\ \lambda_{\mu m}$, so that for $\lambda$ = 0.5 to 1 μm, diameters as small as 2 to 4 m would be adequate. However, because coronagraphs typically only provide good transmission at angles larger than a few (i.e. 2- 4) $\lambda/D$ of the stellar position [1], the estimated aperture sizes must be scaled up accordingly, resulting in most cases in telescope apertures of order 8 - 10 m. Such sizable apertures remain a challenge for space-based systems. Some recent coronagraph designs allow access to somewhat smaller angles [1], and so reduce the telescope diameter requirement somewhat, but extreme telescope accuracy requirements remain. With an exo-earth reflecting roughly $2 \times 10^{-10}$ of the stellar flux in the optical, the necessary wavefront correction level is at the 0.1 nm level [2]. This contrast-based constraint cannot be eased, but it may be possible to obviate the telescope accuracy requirement by instead providing an extremely accurately corrected wavefront downstream in the optical train. This paper explores this approach.

## 2. TELESCOPES

Although telescopes have long been central to astronomy, specific telescope implementations have evolved to meet changing needs. Thus, lens-based telescopes have largely been replaced by reflective telescopes to provide broadband performance, and single-point imaging solutions, such as paraboloidal and dual-mirror Cassegrain and Gregrorian telescopes, have given way in some cases to wide-field imagers such Ritchey-

Chretien and Schmidt telescopes. It is thus natural to ask what type of optical system might be best for high-contrast, narrow-field imaging. To date, coronagraphic "backends" have been appended to existing telescopes. Here we ask whether a different telescope configuration can provide performance superior to that of the more classical telescope/coronagraph combinations.

The first requirement for high-contrast narrow-field imaging is high angular resolution, implying large apertures or baselines. However, filled apertures are not required – only long baselines within some aperture envelope. Second, to allow for deep stellar suppression, a nearly perfect wavefront is required. However, this highly accurate wavefront is not required throughout the optical train; it is required only at the coronagraph entrance. Third, the detection of faint companions requires reasonably high-quality imaging, but not extremely high image quality. Finally, imaging is required only over a very small field of view (FOV), because the region of interest for planetary companions is only a few arc seconds across.

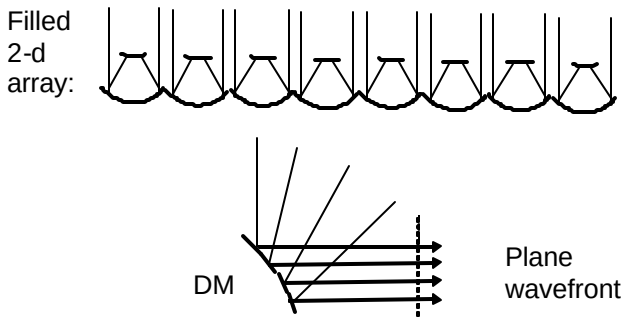


Figure 1. Top: A 2-dimensional "envelope" pupil aperture filled with an array of small telescopes. Bottom: Assembly of a wavefront from an array of sub-pupils with a generalized DM.

The high-quality wavefront is thus required only at the coronagraph entrance. Since an adaptive optics (AO) system will in any case be employed just prior to the coronagraph to apply wavefront corrections, one can consider simply abandoning the attempt to maintain a nearly-perfect wavefront through the bulk of the optical train, focusing instead on correcting or "assembling" a nearly-perfect wavefront for the first time at the AO system output. We thus consider a generalized wavefront "corrector" to assemble a pupil plane wavefront from its constituent pieces, such as individual subpupils. The pieces of the final wavefront need not even arrive from the same direction, since each element of a generalized deformable mirror (DM) can in principle supply its own tip-tilt angles as well as an optical path difference (OPD). As shown in Fig. 1 (bottom), such an optic could thus be used to assemble a pupil plane wavefront from a set of sub-aperture beams (each of which could have high internal wavefront quality).

Where then do the sub-aperture beams originate? Perhaps the simplest case is that of a close-packed array of small telescopes filling a larger "envelope" pupil, as in Fig. 1 (top). Hereafter this case is referred to as a multi-aperture telescope (MAT). The reason for considering this case is that the massive and voluminous monolithic telescope assembly can be replaced by a large number of smaller and more compact telescopes. Thus e.g., an 8 – 10 m primary mirror, with a secondary 10 – 20 m away, can be replaced by a large number of small telescopes of order 10 cm in diameter, each of which provides one sub-aperture beam to the corrector stage. Furthermore, each sub-aperture beam can be matched to an individual DM element, thus providing tip/tilt and OPD matching between neighboring beamlets.

## 3. OPTICAL PATHLENGTH MATCHING

This approach will work only if all of the sub-aperture beams can be phased properly. "Phasing" is normally provided by the monolithic telescope itself, as a telescope can be considered to be a wide-aperture delay line, in which the macroscopic mirrors provide each ray entering the aperture with just the right path delays to arrive at the common focus with a common OPD. (This condition ideally applies only to a single image point, with aberrations increasing as the image point departs from the optical axis.) In the MAT case, OPD matching across the final pupil needs to be achieved in some other fashion.

One could consider using separate delay lines for each compressed sub-aperture beam, but this results in a bulky and complex system of $N^2$ delay lines for an $N \times N$ array of sub-apertures. However, there is an easier way: matched single-mode fibers can be used to provide the necessary OPD delays without a complex system of delay lines, as illustrated in Fig. 2. In principle the small telescopes can be on- or off–axis paraboloids, two mirror systems, or even a set of achromatized lenses. Such a fiber-based approach could even eliminate the need for secondary mirrors in the small telescopes, as single mode fibers can couple directly to primary beams of small focal ratios (F#'s). The approach pursued here thus replaces the macroscopic telescope with an array of small telescopes and a fiber array bundle which is used to assemble the full envelope pupil downstream.

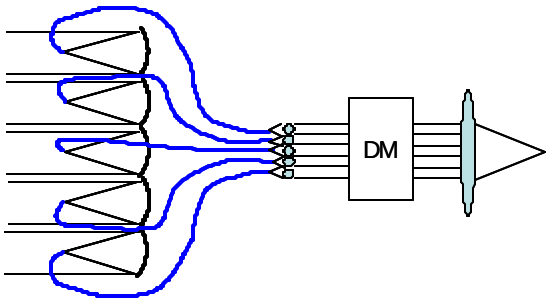


Figure 2. The multi-aperture telescope (MAT) concept: a close-packed array of small telescope-lets is followed by a lenslet array coupled to a fiber array which is used to assemble and phase the pupil.

The accuracy requirement originally levied on the telescope surface is thus transferred to the fiber array. Thus, beamlet OPD, dispersion, intensities, and polarizations must be matched. Thus getting a MAT to work to high precision relies entirely on the degree of matching of the fiber array. A degree of dispersion compensation has already been demonstrated by using macroscopic dispersion compensators to correct for temperature-induced dispersion in the fibers used in long-baseline interferometry [5]. On the other hand, rather than using dielectric wedge compensators, two successive fibers of differing materials might be employed. Conversely, temperature can be used directly as a control element, as can other physical effects, such as stress. Moreover, it is now possible to make use of a wide variety of novel photonic fibers with structurally determined properties, making low-dispersion fibers physically realizable [6]. Thus, while OPD matching for such an array of fibers needs to be demonstrated, it is not viewed as an insurmountable challenge. In contrast, the control systems for the other parameters are fairly straightforward: intensity control can easily be achieved by changing the pointing of the beams onto the individual fiber heads (and so the coupling into the single mode fibers), while polarization control can be achieved by either rotating the fiber ends, or by twisting the fibers.

## 4. COMPARISON TO MONOLITHIC APERTURES

Arrays of subpupils within a larger telescope aperture have previously been considered mostly in the context of pupil plane interferometry [3], but this approach has in general not been considered for direct imaging, likely because of the small field of view (FOV) provided by single mode fibers: for small telescope-lets of diameter of 10 to 20 cm, and wavelengths of 0.5 to 1.0 μm, the single-mode FOV is of order 1 arcsec. However, such a small FOV is not a limitation when the target fields themselves are small, such as in the exoplanet case. Moreover, small sub-aperture diameters also allow coupling of individual sub-aperture beams to individual DM elements (10 cm subapertures within a 10 m envelope pupil would require a 100 x 100 DM), for complete control of subaperture phases. The most significant potential limitation of such a fiber-based imaging system is thus the necessary degree of OPD and dispersion matching of the fibers, but the necessary accuracy is no worse than that needed by a precise monolithic telescope followed by a high-order extreme AO system.

The MAT concept thus replaces a large classical telescope with an array of small telescope-lets situated in a common pupil plane, after which a fiber bundle is used to assemble a compressed and phased pupil. The bulky monolithic telescope primary mirror is thus replaced by a set of light- weight individual telescopes, and the telescope surface accuracy requirement becomes a requirement on phasing the individual sub-apertures. Moreover, the distant secondary mirror and its support structure are eliminated entirely. In place of the voluminous 3-dimensional telescope assembly present in the monolithic case, the MAT optical assembly is much smaller in height, and would be closer to a 2-dimensional structure. For a monolithic telescope of pupil area $D^2$, where D is the primary mirror diameter, its height is FD, where F is the primary focal ratio, (of order 1 - 2), leading to a volume $\approx FD^3$. On the other hand, an array of small telescopes would also fill an envelope pupil of approximate area $D^2$, but the height would be $\approx$ fd, where f is the focal ratio of the small sub-aperture telescopes (again of order 1 – 2), and d is the diameter of an individual sub-aperture telescope, leading to a volume $\approx fdD^2$. Thus, assuming similar focal ratios in the two cases, the height of the required optical assembly is reduced in the MAT case by the factor d/D. Since d/D can be of order 0.01, a very significant savings in volume and weight can result

Note that some variants of the idea of using sub-apertures within a larger telescope pupil have been considered [3], but usually in the context of interferometric pupil-plane recombination. As such, these approaches neither suggested eliminating the monolithic telescope, nor do they yield an image plane. Another concept, the "hypertelescope," does make use of multiple apertures, but these are generally widely separated, and so this approach resembles long-baseline interferometry more than single aperture imaging [4]. In contrast, in the MAT approach, the monolithic telescope is eliminated entirely, the envelope pupil aperture is closely filled with sub-apertures, and a final image plane is directly provided.

## 5. THE EFFECT OF SINGLE MODE FILTERING

In the MAT approach, the overall "envelope" pupil is modified in several ways – it is first segmented into an array of sub-apertures with small gaps in between, then each sub-aperture is individually spatially filtered, leading to a perfect wavefront in each sub-aperture. Finally, the spatially-filtered sub-apertures are assembled into a composite pupil and phased. In the first step, the pupil is in effect "digitized." In the second step, only the average field in each sub-aperture is transmitted down its fiber. Propagation down the fiber removes higher order aberration modes [7], leading to a perfect plane wavefront in the emerging recollimated sub-aperture

beam. The net result for the final assembled, collimated pupil is thus a "digitized" pupil, with the field in each sample given by the average field coupled into that fiber.

Nevertheless, the image at the focus of the final, common focusing optic is little affected by this digitization. With non-zero gaps between the subapertures, small differences between the monolithic pupil point spread function (PSF) and the MAT PSF arise. The extra scattered light ends up at large angular offsets from the optical axis, in particular, at multiples of $\lambda/g$, where g is the grid or "grating" spacing. Thus, the first grating sidelobe due to the gaps lies outside the subaperture single mode beam (of FWHM $\approx \lambda/d$, where d is the subaperture diameter). As a result (Fig. 3; left), the inner part of the PSF, i.e., that part which couples to the single mode fiber beam, is not very different from the original monolithic telescope PSF (unless the gaps are a large fraction of d).

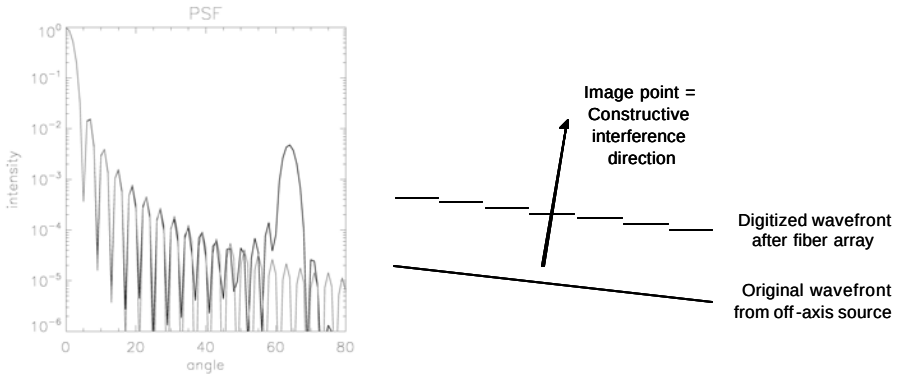


Figure 3. Left: Comparison of the diffraction patterns produced by a monolithic circular aperture (light curve), and the same aperture divided into an array of subapertures (dark curve). The central dark hole region (corresponding to the single mode subaperture beam) extends out to "angle" = 32, well inside the first PSF replica at "angle" = 64. Right: The effect of spatial filtering on the wavefront from an off-axis point source is to digitize each subaperture field at its average value.

Now, single mode fibers couple only to light within their input numerical apertures, thus providing an outer working angle (OWA) on the sky roughly equal to half the subaperture diffraction beam width, or $\lambda/2d$. Sources much beyond the OWA are thus inaccessible to observation with a single-mode filter based system. However, only a small FOV is desired in the exoplanet case. In fact, the domain of influence of the DM is perfectly matched to this OWA if an N x N DM array were to be matched to the N x N subaperture array because $N\lambda/D = \lambda/d$. Since this N x N central region of the focal plane defines the well-corrected "dark-hole" region, beyond which AO correction does not apply, the use of individual single-mode-filtered subaperture beams of FWHM $\lambda/d$ implies no loss of information in the targeted inner dark hole. Furthermore, the extra scattered light discussed above is well beyond $\lambda/2d$, or outside of the dark hole region, and so is irrelevant.

For an off-axis source, the phase digitization leads to a "staircase" phase distribution at the output of the fiber bundle (Fig. 3; right). Nevertheless, constructive interference, and so the image point, occurs at the angle for which the phase steps are all in phase, i.e., in the original image direction. Thus, within the DH, the imaging remains true even after passage through the fiber array. The use of an array of single-mode-filtered subapertures thus provides a system optimized specifically for the narrow-field imaging case: the single-mode subaperture FOV corresponds exactly to the well-corrected DH region, and also to the source region of interest. Conversely, there is little interest in the region beyond the fiber OWA, because of the lack of both DM correction and companions of interest. Matching the sub-apertures to the DM elements thus guarantees that only the desired central dark hole is imaged properly.

## 6. STELLAR SUPPRESSION

The final aspect is starlight suppression. Many orders of magnitude of starlight suppression are needed to allow detection of faint planetary signals. One of the great advantages of the fiber-based MAT approach is the ability to provide arbitrary attenuations in each of the subapertures (Fig. 4; left), thus allowing the pupil to be apodized simply by adjusting the amount of light emerging from each of the fibers. This can be accomplished by slightly mis-pointing the input beams to slightly decouple each starlight beam from its fiber. As this makes use of hardware already needed for intensity control, no additional hardware is needed for pupil apodization. The resultant apodization is digital, but as can be seen in Fig. 4 (right), this does not yield significant PSF changes from the apodized monolithic telescope case. Moreover, a number of different coronagraphs can also be realized: for example, several of the outer subpupils can be "turned off" to generate square, circular, or arbitrarily shaped pupils [1]. (Because these pupils will in fact be digitized versions of the idealized shapes, pupil shapes with very fine structures will not be reproduced faithfully.) Furthermore, since the phase of each sub-aperture beam can in principle also be adjusted arbitrarily, any arbitrary pupil plane intensity and phase apodization can potentially be applied by means of a fiber bundle. Thus such a "digital coronagraph" (DC) has a great deal of flexibility, an aspect which has been missing in prior coronagraphic designs. Of course, the pupil can be assembled in any geometry desired simply by translating the fiber outputs laterally. The exit pupil distribution can then be arbitrarily redefined (e.g., Fig. 5; left), allowing a host of possibilities for the remapped pupil, such as a digitized version of "phase-induced amplitude apodization" [8], but without the need for precise high-order optical surfaces.

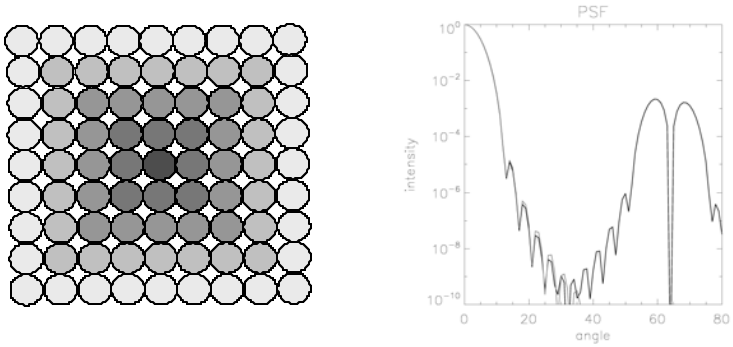


Figure 4. Left: Pupil apodization by intensity control of the pupil subapertures. Right: Comparison of the PSFs produced by a $\cos^4(\pi r/2r_{max})$ apodization applied to a monolithic circular aperture (light curve), and a digitized version of the same pupil (dark curve). Within the OWA of the individual sub-aperture single-mode beams (to "angle" = 32), very little difference between the curves is seen.

Moreover, the MAT approach is also a natural match to "nulling coronagraphs" [7], which rely on the lateral shearing and re-combination of light from different regions of the pupil. In fact, such nullers can be considerably simplified by means of a MAT, since such nullers already rely on an array of single mode fibers coupled to individual DM elements in the "back-end". The MAT concept allows extending this downstream pupil segmentation all the way back to the input pupil. Thus, in the simplest case, the nuller's fiber array needs only to be mapped to the input fiber array. On the other hand, it is possible to go a step further to combine the two ideas more seamlessly. In particular (Fig. 5; right), rather than using macroscopic shear to superpose different parts of the aperture, one can instead simply rearrange the outputs of the input fibers so as to co-locate and intermingle the desired portions of the pupil next to each other. Then for example, four newly-adjacent beams can be directly combined in a fiber nuller [9,10], without any intervening optics or beamsplitters (Fig. 5; right).

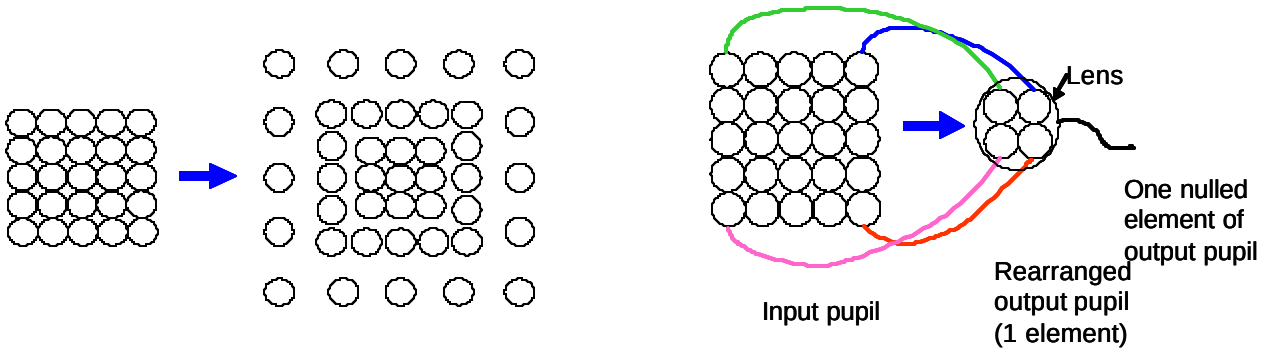


Figure 5. Left: Pupil remapping by relocation of the subaperture fiber outputs. Each fiber can also have its intensity and phase adjusted arbitrarily. Right: A 2nd example of pupil remapping, in which the fibers are interwoven, simulating the effect of lateral beam shear. Each set of 4 fibers can then be combined at a fiber nuller without the use of any beamsplitters.

## 7. SUMMARY

The approach to direct detection of faint planetary companions to bright stars discussed here eliminates the high-accuracy monolithic telescope assembly in favor of a close-packed array of small telescopes. The envelope pupil of these subapertures is assembled by means of a single-mode fiber array, and the resultant digitized pupil allows for the natural implementation of a variety of coronagraph types. The MAT digital coronagraph is a very new idea, and so not all cases have been explored extensively yet, but the approach shows great potential, both because of the variety of coronagraphs enabled, and because the approach can be extended to any envelope pupil diameter, allowing space-based MATs of arbitrarily large collecting area in the future. The MAT approach also potentially greatly relaxes the volume, mass, and cost constraints thought to apply to high-contrast telescope/coronagraph systems based on large and expensive monolithic telescope assemblies, thus perhaps providing a more feasible route to TPF-C or to a potential precursor mission. The next steps clearly call for demonstrating such a novel MAT digital coronagraph in the lab, after which a digital coronagraph can be implemented on a ground-based telescope and/or on a small space-based mission. All of this is of course subject to funding, but this promising new approach is ripe for exploitation, and thus requires only support.

This work was carried out at the Jet Propulsion Laboratory, California Institute of Technology, under contract with the National Aeronautics and Space Administration.

[1] O. Guyon, E.A. Pluzhnik, M.J. Kuchner, B. Collins & S.T. Ridgeway, Astrophys. J. Supp. 167, 81 (2006).
[2] F. Malbet, J.W. Yu & M. Shao, Publ. Astron. Soc. Pac. 107, 386, (1995).
[3] S. Lacour, E. Thiebaut & G. Perrin, Mon. Not. Royal Astron. Soc. (2007), in press.
[4] A. Labeyrie, Astron. & Astrophys. Supp. 118, 517 (1996).
[5] T. Kotani, G. Perrin, J. Woillez, J. Guerin & G. Maze, in Proc. SPIE Vol. 5491, New Frontiers in Stellar Interferometry, ed. W.A. Traub (2004), p. 647
[6] A. Ferrando, E. Silvestre, P. Andres, J.J. Miret & M.V. Andres, Optics Express 9, 687 (2001)
[7] B. Mennesson et al., in Proc. SPIE Vol. 4860, High-Contrast Imaging for Exo-Planet Detection, ed. A.B. Schultz & R.G. Lyon (2002), p. 32
[8] O. Guyon, Astron. Astrophys. 404, 379 (2003)
[9] O. Wallner, J.M.P. Armengol and A. Karlsson 2004, in Proc. SPIE 5491, 798
[10] P. Haguenauer & E. Serabyn. 2006, App. Opt., 45, 2749.